

FUDMA Journal of Sciences (FJS) ISSN online: 2616-1370 ISSN print: 2645 - 2944 Vol. 9 No. 10, October, 2025, pp 277 – 289

TRAM JOHNES OF THE PARTY OF THE

DOI: https://doi.org/10.33003/fjs-2025-0910-3856

STRUCTURAL AND MINERALISATION MAPPING OF MUSCOVITE ORE DEPOSITS IN ELEEKU, SOUTHWESTERN NIGERIA

*¹Magaji Yusuf, ¹Folorunso O. Ismaeel, ²,³Salaudeen A. Salaudeen, ³Olajide A. Temitayo and ⁴Wahab Owolabi Folorunsho

¹Department of Geophysics, University of Ilorin, Ilorin, Nigeria.

²Department of Physics with Electronics, Ahman Pategi University, Patigi, Nigeria.

³Department of Pure and Applied Physics, Ladoke Akintola University of Technology, Ogbomoso, Nigeria.

⁴Geological Technology Department, Federal Polytechnic Offa, Offa, Nigeria.

*Corresponding author's email: <u>21-68gp003.pg@students.unilorin.edu.com</u>

ABSTRACT

Aeromagnetic data has been successfully adopted to characterise mica mineralisation for industrial purposes in Eleeku, Nigeria. The data, sheet 223-Ilorin on a scale of 1:100,000 were obtained from the Nigerian Geological Survey Agency (NGSA) at a height of 80 meters along a series of NE-SW flight lines spaced 500 m interval. The Total Magnetic Intensity data was gridded at 125 m then reduction to the magnetic equator (RTE) was applied to center magnetic anomalies over their respective magnetic source bodies with the aid of Oasis MontajTM software. Other enhancement techniques applied are total horizontal gradient (THG), tilt angular derivative (TDR) and 3-D Euler deconvolution. The results of the highest peak of THG on zero TDR in addition to 3D Euler deconvolution serve as source edge detection of geologic structures responsible for hosting mineralisation. 15 faults oriented in NW-SE and NE-SW directions were discovered. 4 out of these 15 are carriers of muscovite bearing faults, with a maximum depth of approximately 600 m and dip angles varying between 65° and 82°. 3D Euler deconvolution of 0 structural index at a grid cell of 125 m and a window size 16x16 helped determine depth, position and contact between two lithologies of different magnetic source bodies. The maximum depths and dip angles to the top of the source bodies ranging between 450m - 1200 m and 65° - 82° respectively were found in Gudugba and Aboto Alfa communities while the shallow source depths and dip angles ranges from 300 - 400 m and 18° – 64° were identified at Eleeku, Igbona and Oloro areas. Based on these results, fault with depths range of 50 m - 600 m coincide with areas where muscovite- bearing faults were found within the outcropping basement rocks of Eleeku area at (08° 10' 26.06"N 004° 35' 44.69"E) of high magnetic signatures.

Keywords: Aeromagnetic Data, Oasis Montaj, Euler Deconvolution, Tilt Angle Derivative, Eleeku

INTRODUCTION

The Eleeku pegmatite is thought to have the ability to mineralize both metallic and industrial materials including tantalite, muscovite mica and gemstones because the veins are often obscured by weathered schist and are occasionally exposed by erosional structures (channels and gullies). The possible occurrence of mineralisation in this area is primarily within the veins and linear structures thereby the application of the aeromagnetic method in delineating them in terms of depth, trend and aerial extent is very essential since geologic structures such as dykes, folds, joints, faults are responsible for the emplacement of ore deposits on account of tectonic activities and hydrothermal fluid circulation.

Geophysical technique has been found very useful in mineral exploration. It involves studying the physical properties of the earth to provide vital information on subsurface material conditions for numerous practical applications. These are done by taking measurements at or near the earth's surface that are influenced by the internal distribution of physical properties (Durrheim and Cooper, 1998). Structures such as dykes, Folds, joints, faults are responsible for the emplacement of ore deposits on account of tectonic activities and hydrothermal fluid circulation. An aeromagnetic geophysical technique has been widely used for geophysical and geological survey since its inception. The most distinguishing feature of this technique, compared with other geophysical techniques, is the rapid rate of coverage and low cost per unit area surveyed. The use of this technique makes it possible for geophysicists to acquire data regardless of ownership or accessibility of remote lands of interest.

The most important and accurate information provided by magnetic data is the identification of the structural fabric of the basement rocks, consistent discontinuities, and/or pattern breaks in the magnetic fabric (Balogun, 2019; Bassey and Barka, 2015; Osagie et al., 2021). It is also a fast, economical and versatile geophysical tool for delineating subsurface geological structures and rocks in areas with poor exposure (Lawal, 2020; Magaji and Sanusi, 2021; Usman. et al., 2014). The magnetic method is essential for mapping pegmatite because some pegmatites contain magnetic minerals such as magnetite or by the host rock's magnetic properties, which create magnetic anomalies in the Earth's magnetic field that can be detected and mapped from the surface, or which may be influenced by the geological processes that also formed the rare earth element (REE)-rich pegmatites. This allows geophysicists to locate and understand the geometry of hidden or deeply buried pegmatite bodies, especially in areas with weathered overburden, aiding in the exploration for muscovite and rare metals like lithium (Li), Niobium (Nb), Tantalum (Ta), Tin (Sn), Ceasium (Cs), Tungsten, Columbite and Beryllium (Be). Muscovite and these metals are essential in modern technology, including rechargeable batteries, electronics, construction, casting, galvanizing, production of containers, metal wears, and specialized industrial applications (Okunlola, 2005; Adekoya et al., 2003; Garba, 2003; Okunlola and Ogedengbe, 2003; Okunlola and Jimba, 2006; Okunlola and Somorin, 2006; Okunlola and Ofonime, 2006).

Various techniques, based on the frequency analysis of the magnetic field, have been established to define parameters

such as location of boundaries and depths of the magnetic rocks that cause anomalies in the magnetic field (Salem et al., 2008). The horizontal gradient magnitude is one of such methods used for locating contacts and faults from magnetic anomaly data (Cordell & Grauch, 1985; Philips, 2000). Other methods for location of source boundaries and depth estimates include euler deconvolution (Nabighian, 1972; Roest et al., 1992) and tilt derivative (Miller & Singh, 1994; Verduzco et al., 2004). The analysis of aeromagnetic data using derivative methods is to provide an indirect means of seeing the subsurface by sensing various magnetic properties of rocks (Salaudeen et al., 2025). The work of Aliyu et al., (2020) stated that high magnetic signatures of magnetic survey at basement region are considered to be minerals with high magnetic susceptibility which are columbite and tantalite while regions with low susceptibility are sandstone, quartz, graphite and feldspar. Their results suggest that this method can be applied to detect minerals presence in pegmatite of which muscovite (mica) is one. Aeromagnetic survey data can be used to unravel the subsurface geological evidences which are related to rare earth element (REE) enrichment in pegmatite field (Ishola et al., 2020). In this study, we examine the aeromagnetic anomaly data and attempt to identify subsurface geologic structures that may be important in future mineral exploration. Thus, the objectives of this work are to identify the location, edges and source depth from images using 3-D Euler Deconvolution, TDR and THG of possible muscovite- bearing faults in Eleeku area.

Geographic Location and Geomorphology of the Study Area

The study area, Eleeku is situated at the southwestern part of the topographic sheet of 223 (Ilorin) Nigeria. The location of the site is bounded by the geographic coordinates between longitudes of 004°30′ 00″ E to 004°40′ 00″ E and latitudes 008°16′ 00"N to 008° 04′ 00"N covering a total area of approximately 3,080.25 km² (Figure 1). It lies in the 31N (Minna Datum) coordinate system of Universal Traverse Mercator corresponding to Northings of 885000 mN and 955000 mN and Eastings of 667000 mE and 730000 mE. It is a gently sloping area, with heights ranging from 247 m above sea level on the southern margin to 235 m within the stream channel at the northeastern side. The geology of Eleeku and soil belong to the Precambrian rocks, which include porphyritic granites, pegmatite, biotite and hornblende gneiss as shown in (Figure 2). They make up a portion of the Craton of West Africa that is essentially comparable to other basement rocks in southwest part of Nigeria that have been the focus of study (Oluyide, 1988; Oyawoye, 1972; Rahaman, 1988, 1989). They also include a migmatite structure that is Eburnean (2000-200 Ma). Intense magmatic activity led to the deposition of the Older Granite series of Pan African age in the area (Ajibade et al., 1987; Dada, 1998; Turner, 1983).

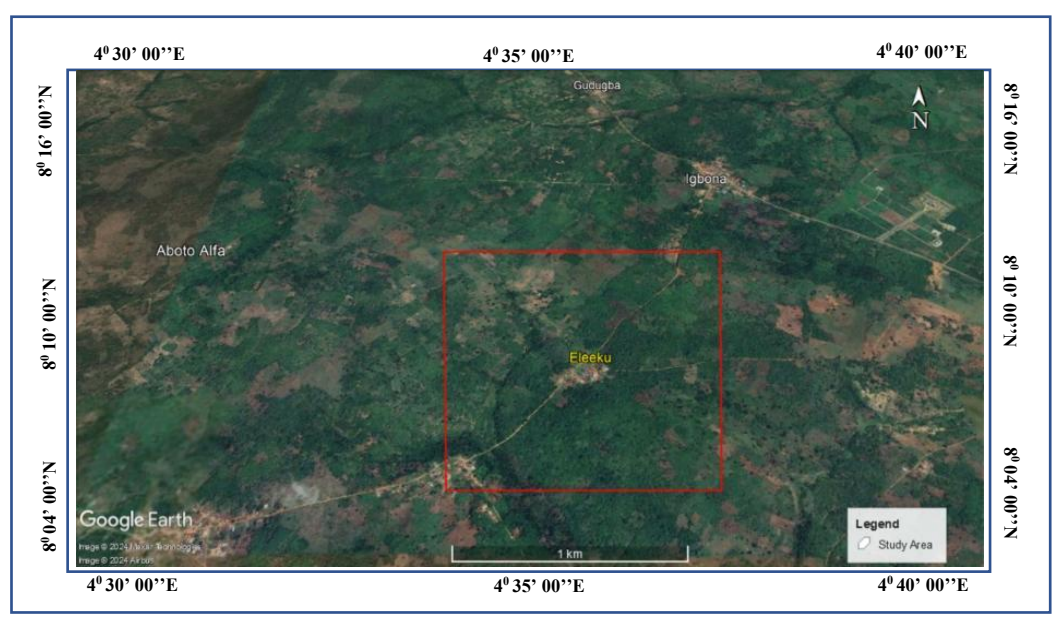


Figure 1: Google Earth Map of Eleeku Area

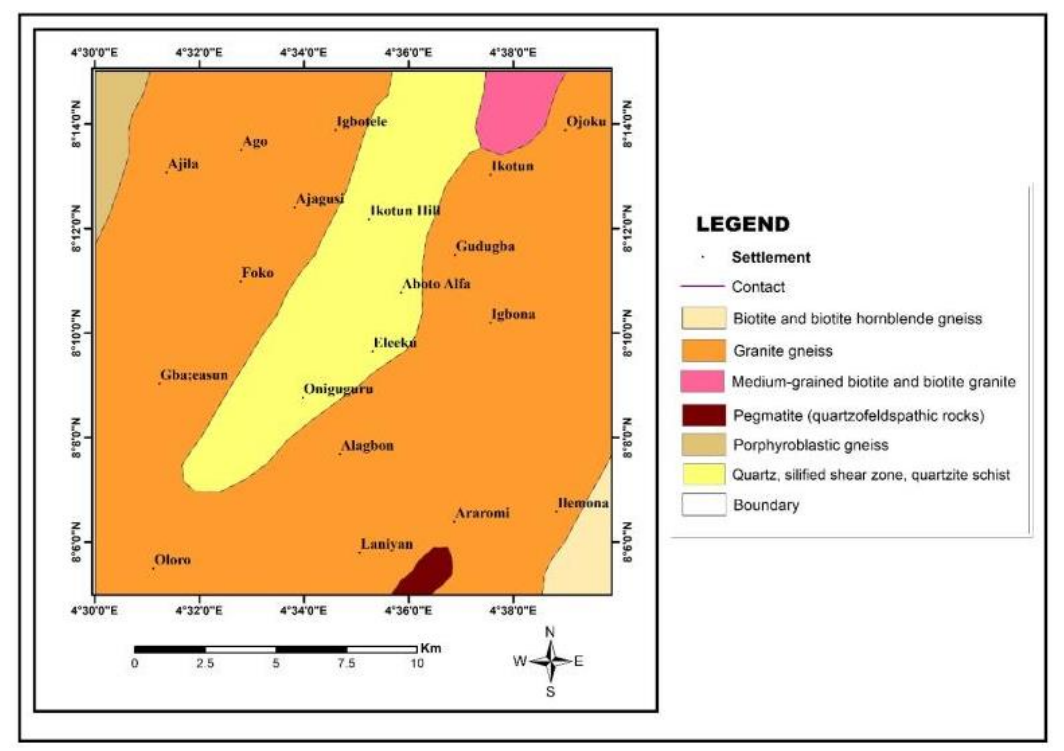


Figure 2: Geological Map of Eleeku (Adapted from NGSA, 2023)

Steep weathering depth and lateritic surface and near-surface subsoil are features associated with locations underlain by mica schist. The aforementioned well reached red lateritic soil that was roughly 10 m thick. The presence of exposed veins of pegmatites buried beneath and cross cutting through weathered mica schist along an erosion-created channel, large amounts of quartz and feldspar boulders at multiple locations, and a shallow pegmatite ridge across the site suggest that the mica schist is pegmatite.

MATERIALS AND METHODS

Data Acquisition

The aeromagnetic data bounded by latitude 08° 00′ 00″ N to 08° 30′ 00″ N, and longitudes 004° 30′ 00″ E to 005° 00′ 00″ E was obtained from the NGSA (Nigerian Geological Survey Agency). The data was acquired at a height of 80 meters along a series of northeast-southwest flight lines spaced 500 m interval. The data were made available in ½ degree sheets and in maps contoured at a 1:100,000 scale. The data were digitally recorded in a text file of (X, Y, Z) and subsequently interpolated to form a grid of 55x55 with 500 m spacing. The Z denotes the magnetic field intensity, expressed in nanoteslas

(nT), X stands for longitude and Y for latitude of the study area expressed in metres (m).

Data Processing

The Total Magnetic Intensity (TMI) is the combination of geomagnetic and strength of the crustal and fields. The NGSA removed the effect of geomagnetic field from the aeromagnetic data by applying the International Field of Geomagnetic Reference point (IGRF). Figure 3 shows the corrected map of Eleeku TMI. Methods of different standard derivative and match filtering were applied on the TMI anomaly map of the study area for better improvement of subsurface geologic structural image. Oasis Montaj (GeosoftTM) is the commercial software package used for the processing of all the data. The uncertainty in the findings from match filtering and derivative-based approaches necessitates the use of different filters where each is highlighting a particular aspect of the aeromagnetic anomaly data, to evaluate whether the findings are consistent or contradictory (Sherif, 2010). Should the former be true, there is increasing assurance that the findings carry some meaningful significance for the subsurface geology.

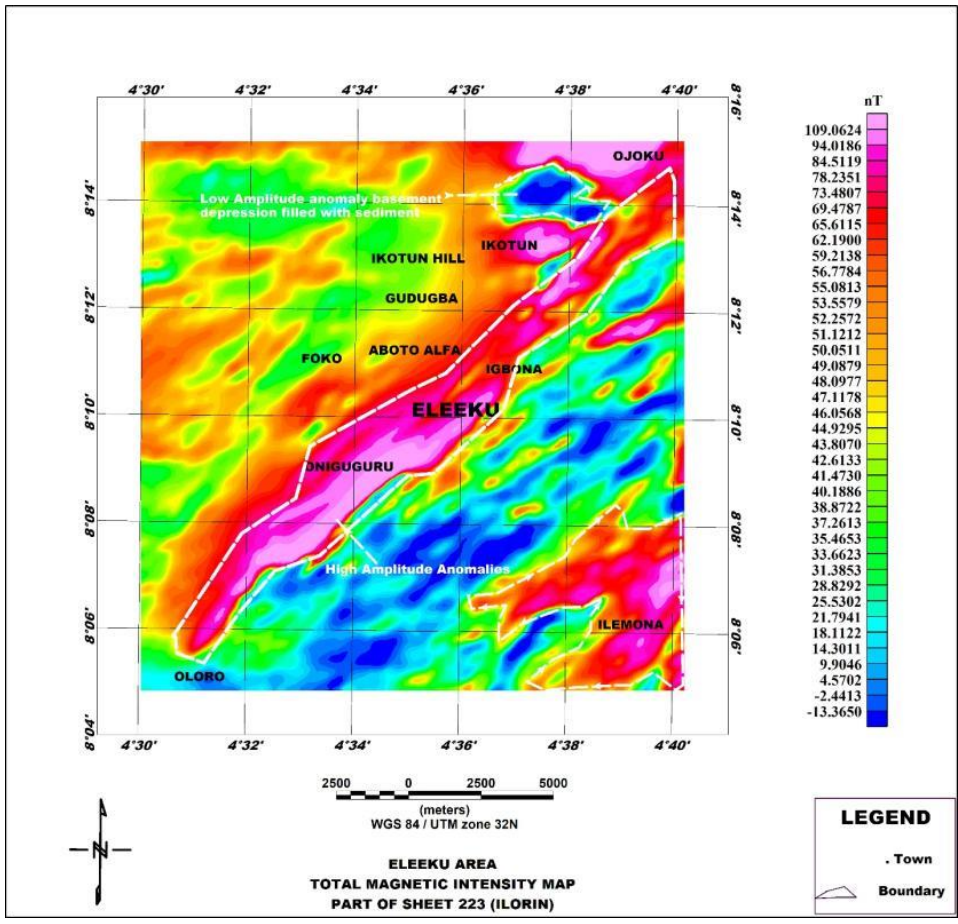


Figure 3: Colour-Shaded TMI Map of Eleeku Area

The reduction-to-equator (RTE) filter was first used to address the displacement of magnetic anomalies from their sources at non-polar and non-equatorial latitudes by centering these anomalies directly over their origin points and is also effective for regions of low latitude, assuming the effect of observed magnetic field is as a result of induced magnetic effects (Reid et al., 1990). The lack of volcanic rocks in the area supports the theory of induced magnetization and the variables require for applying of the reduction-to-equator (RTE) filter are the TMI of the study area inclination and declination. (Durrheim and Cooper, 1998) suggested that pole reduction is difficult at low magnetic latitudes, since some bodies have no detectable magnetic anomaly at zero magnetic inclination.

Total Horizontal Derivative (THD) Method

One of the effective tools for identifying the edges and the horizontal extent of magnetic source bodies in Eleeku area is edge detection technique, this method could reveal the magnetic sources and locations where the Eleeku schist was disrupted by faulting. The THD of the magnetic field are the combination form of the magnitude of the horizontal gradient in a given direction which maximize lateral changes and reduce the regional trend in that direction. The derivative usually attains highest in the regions where the magnetic susceptibility difference is highest, however this identifies the boundaries of geologic structures and shows discontinuity perpendicular to the direction of derivation (Cordell and Grauch, 1985; Roest and Pilkington, 1993). A simple method to highlight potential boundaries of subsurface magnetic source bodies is to identify the maximum horizontal gradient. The alignment of highest horizontal gradient indicates a linear

contrast in magnetic properties that signifies the edge of a magnetic source body.

Therefore, this method entails identifying locations where the local peak in the HGM align thereby indicating the edges of magnetic source bodies. It should be noted that these maxima are most pronounced when the edges are vertical, while edges that significantly deviate from the vertical do not generate local gradient peak. The HGM method is not sensitive to noise in the magnetic data since it needs to compute the two firstorder horizontal derivatives of the magnetic field (Phillips, 2000). Considering that M (x, y) represents the total magnetic intensity at a point (x, y), the HGM can be expressed as:

$$HGM_{(x,y)} = \left[\left(\frac{\partial M}{\partial x} \right)^2 + \left(\frac{\partial M}{\partial y} \right)^2 \right]^{\frac{1}{2}}$$
 (1)

$$\begin{split} & \text{HGM}_{(x,y)} = \left[\left(\frac{\partial M}{\partial x} \right)^2 + \left(\frac{\partial M}{\partial y} \right)^2 \right]^{\frac{1}{2}} & \text{(1)} \\ & \text{where } \frac{\partial M}{\partial x} \text{and } \frac{\partial M}{\partial y} & \text{denotes the horizontal derivatives of the} \end{split}$$
aeromagnetic data.

The RTE grid data from the study area was utilized to compute the HGM, and peaks were located by moving a 3x3 window over the grid to identify the highest points (Blakely and Simpson, 1986).

Tilt Angle Method

The use of the TDR method in exploration especially solid mineral is primarily for delineating geological structures at shallow source, this technique stands out due to its remarkable efficiency in detecting the boundaries of magnetic source bodies. The technique was defined and given by (Miller and Singh, 1994; Verduzco et al., 2004) as:

$$\theta = TDR = tan^{-1} \frac{(FVD_{(z)})}{(HGM_{(x,y)})}$$
 (2)

Where

Total Horizontal Derivative = $HGM_{(x,y)} = \left[\left(\frac{\partial M}{\partial x} \right)^2 + \left(\frac{\partial M}{\partial y} \right)^2 \right]^{\frac{1}{2}}$

First Vertical Derivative = $FVD_{(z)} = \frac{\partial M}{\partial z}$

 $\frac{\partial M}{\partial x}$, $\frac{\partial M}{\partial y}$, and $\frac{\partial M}{\partial z}$ denotes the 1st order derivatives of the potential field, M in the directions of x, y, and z.

The tilt angle is the proportion of the vertical to the horizontal derivatives ranging between -90° and +90° (Salem et al., 2007; Verduzco et al., 2004). The horizontal derivative shows the geological features like fault while the vertical derivative reduces the anomaly width. Hence, zero contours i.e. $\theta = 0^{\circ}$ identify the spatial locations of boundary origin where the depth of this origin determined the distance between the zero contour and the -45° or +45° contours (Salem et al., 2007). Inclination makes TDR undergoes significant variation however when the inclination is either 0° and 90°, the zerocrossing position is found to be nearly coincident with the edges of two-dimensional magnetic sources like dikes and blocks (Salem et al., 2007). For the purpose of this study, the reduced-to-equator (RTE) anomaly field is favoured over reduced-to-pole (RTP) transformations, even though both work effectively for the TDR filter, but the RTE field is more closely aligned with the magnetic equator (Salem et al., 2007). When considering the RTE transformation, it is important to note that the total derivative response shows negative amplitudes within the boundaries of magnetic source bodies and positive amplitudes in the surrounding regions beyond the influence of the magnetic sources.

3D-Euler Deconvolution Method

Recently, there has been more recognition in the use of 3D Euler deconvolution, thanks to its automated processes and rapid interpretation for both profile and grid data (Barbosa et al., 1990; Durrheim and Cooper, 1998; Ravat, 1996) This method entails the homogeneous equation, with (Thompson, 1982) showing that Euler's homogeneity relation can be

$$\begin{split} &(x-x_0)\frac{\partial T}{\partial x} + (y-y_0)\frac{\partial T}{\partial y} + (z-z_0)\frac{\partial T}{\partial z} = N(B\text{ -}T) \\ &\text{where } x_0, \ y_0 \ \text{and} \ z_0 \ \text{is the location of the magnetic source,} \end{split}$$

which generates the total magnetic field T measured at (x, y, z), and B denotes regional value of the total magnetic field. N stands for the structural index. Each iteration of the moving window resolves the position and depth of sources by solving a potentially overestimated system of linear equations. The anomaly resulting from the point source and a regional field can be added to form the total field, as shown by equation:

$$(x - x_0)\frac{\partial T}{\partial x} + (z_0)\frac{\partial T}{\partial z} = N(B - T)$$
 (4)

 $(x-x_0)\frac{\partial T}{\partial x} + (z_0)\frac{\partial T}{\partial z} = N(B-T) \tag{4}$ The Euler deconvolution method for depth estimation makes use of the first-order derivative and requires a nature assumption on the source is known as the structural index (Blakely and Simpson, 1986; Mushayandebvu et al., 2001). As a homogeneity factor, the structural index N connects the position of the source to the gradient components the magnetic field. Fundamentally, N measures the rate at which the magnetic field changes with distance from the source, and is closely related to the source dimensions. By modifying N, we can estimate the geometry and depth of magnetic sources. However, Euler deconvolution is applied for boundary detection with depth estimation.

Magnetic interpretation often employs Euler deconvolution since it does not necessitate knowledge of the magnetization vector and needs only minimal previous knowledge of the shape of magnetic source (Thompson, 1982). It has been shown that incorrect selection of structural index is the cause of a wide solution of source locations and significant biases in depth estimation. Reid et al., (1990) proposed that an accurate N results in the most concentrated tightening of Euler solutions around the targeted geological feature.

Based on the type of the body source and the potential field data (magnetic or gravity), the N parameter value changes. This study estimated the depths to the tops of the contacts using standard 3D Euler deconvolution along the positions of structural faults derived from tilt angle derivatives.

Table 1: Magnetic Model of 3-D Euler Deconvolution Structural Indices for Depth Estimation (Oladejo et al., 2020)

Geologic Model	Number of Infinite Dimension	Magnetic Structural Index
Contact	2(x, y, z)	0
Sil	2(x and y)	1
Dyke	2(z and x-y)	1
Pipe	1(z)	2
Horizontal cylinder	1(x-y)	2
Sphere	0	3

With the right choice of structural indices of 3-D Euler deconvolution, cluster solutions that relate to geological structures are produced. Example is a sill forming a cluster near a curvature. a vertical pipe as a point cluster and a dyke as a linear trend (Akinlalu et al., 2018). After performing some calculations and iterating with various window sizes and for the fact that the anomalies of interest are generally between 50 to 1250 meters wide, 1 km search window size was estimated. With a grid cell size of 125 metres, this equates to approximately 16 grid cells. Therefore, the window size for this Euler solution is 16 × 16 while (Whitehead and Musselman, 2008) stated that the 3D Euler deconvolution in Oasis montajTM software allows a maximum window size of 20 × 20 for standard exploration targets

Determination of Fault Dip Angle and Direction

For a geologic contact such as fault trace, the magnetic response of the deepest part corresponds to the maximum upward continuation. When the contact is vertical, the peak values of the total horizontal gradient of the upward continued fields coincide at the same location. However, if these maxima shift horizontally, the direction of the contact dip becomes which allows the angle of fault dip relative to the horizontal to be estimated using the technique suggested by Chiapkin (1969).

By applying upward continuation to the anomalous curves at various height levels, their corresponding total horizontal derivatives was calculated and then the angle α was determined by:

$$\cot \propto = \frac{x}{y} \tag{5}$$

Where x indicates the distance measured along the line between the projection of the horizontal derivative of the curve at height (y) and the projection of the fault trace.

RESULTS AND DISCUSSION Map of Reduction to Equator (RTE) of Eleeku

Figure 4 reveals two main types of magnetic wavelength for colour-shaded map of RTE with intensities ranging from -10.0637 to 103.0797 nT. The amplitude of the magnetic anomalies is categorized into strong, intermediate and weak zones widely distributed across the study area. The filter however centers these anomalies on their magnetic sources thereby simplifying the interpretation of the map.

Weak Anomalies Zone Observed at Different Locations of Eleeku Area

Weak anomalies are noted in the first zone at the northeastern part of Ikotun axis trending in the NW-SE direction. This region at longitude 4° 38' E and latitude 8° 14' is filled with sediment of low negative anomaly basement depression ranging from -10.006 to 14.837 nT. The magnetic anomalies form a distinct band that is oval in shape with a width of about 3.5 to 4.0 km associated with quartz schist and granite gneiss when infer on the geologic map of Eleeku. Large dominant weak magnetic signatures observed at the southern part of Oniguguru to the eastern part of Eleeku with major structures trending in the E-W direction. There is a combination of both

high and low anomalies defined by coordinates 4°36′E to 4°40′E of longitude and 8°08′N to 8°11′N of latitude with magnetic susceptibilities ranging from -10.006 to 49.2429 nT. Within this zone, the NW-SE trending structures suggest an early phase of ductile deformation (event), probably from the Eburnean era (pre-Pan-African).

Strong Anomalies Zone of Eleeku Extending to Ojoku Axis: Northeast — Southwest Direction

The second zone of anomalies which is said to be strong reflect deeper, high frequency and positive anomalies which extend from the northwestern part of Oloro passing through Oniguguru, Eleeku and Igbona axis to the extreme northern part of Ojoku axis. The magnetic anomaly of this signatures defined by coordinates 4°32'E to 4°40'E of longitude and 8°07'N to 8°14'N of latitude range from 57.0368 to 103.0797 nT trending in the NE-SW direction interpreted as quartzite and schist units when inferred on the Eleeku geologic map. It is suspected that these features were formed on the muscovite schist belt at the period of the thrust fault. Anomalies in a Northwest-Southeast direction from the Oniguguru anomalies to Ojoku anomalies.

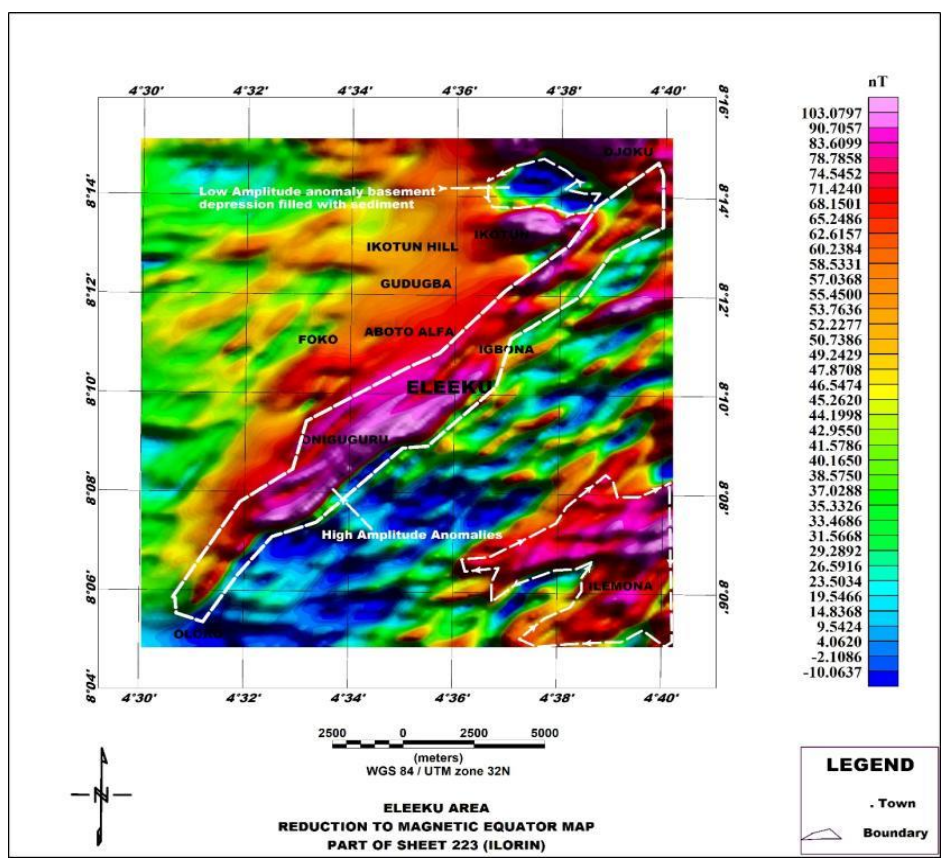


Figure 4: Colour-Shaded Reduction to Magnetic Equator Map of Eleeku Area

Later on, there occurred a phase of deformation characterized by the transition from ductile to brittle, a phenomenon ascribed to the later stages of the Pan-African period (McCurry, 1978) in the regions of high magnetic signatures part of the study area. These areas can be considered to have the same structural formation i.e. the extension of positive values of Eleeku anomalies in a Northwest-Southeast direction from the Oniguguru anomalies to Ojoku anomalies.

Tilt Angle Derivative (TDR) and Total Horizontal Derivative (THD)

This filter is commonly used to delineate and map geologic structures showing shallow basement attributes or areas of interest for mineral exploration. When applied to the RTE anomaly data, the TDR filter bring clearer the resolution of these structural features and displayed magnetic source bodies that align with the overall pattern. With this transformation, one can horizontally pinpoint and measure the width of the boundaries of magnetic source bodies of the area. Different

magnetic source anomalies were revealed on the map with their values ranging from -1.3725 to 1.3892 radian. High positive magnetic anomalies depicted in orange, red and pink colours appeared outside magnetic bodies range from 0.2498 to 1.3892 radian while low negative magnetic ones appeared in blue and green colours occurred over magnetic source bodies range from -1.3725 to 0.2498 radian.

On the map, zero contours signify the positions where magnetic susceptibilities sharply change within the magnetic source bodies of high and low anomalies. These zero contours denoted by the green to yellow colour change, therefore represent the contact boundaries of the magnetic source bodies. It also reveals magnetic source bodies that align with the overall pattern observed in the RTE map. From the

southwestern side of Oniguguru axis to the northeastern part of Igbona area, the magnetic source bodies are linear. Starting from Eleeku to Igbona, the source bodies appear more massive. In addition, the Eleeku fault is evident as a prominent discontinuity that cuts through the map with TDR magnetic signatures ranging from 0.9975 to 1.3892 radians. The map of TDR indicates that the rocks in the area appear to have experienced probably two nearly spaced deformation cycles. These episodes include the early event 1 episode (Figure 6) defined the Eburnean period and connected the recent period 2 Episode attributed to the Pan African period. Also, the application of HGM on the RTE data of Eleeku (Figure 7) is another alternative method for detecting the edges of magnetic structures.

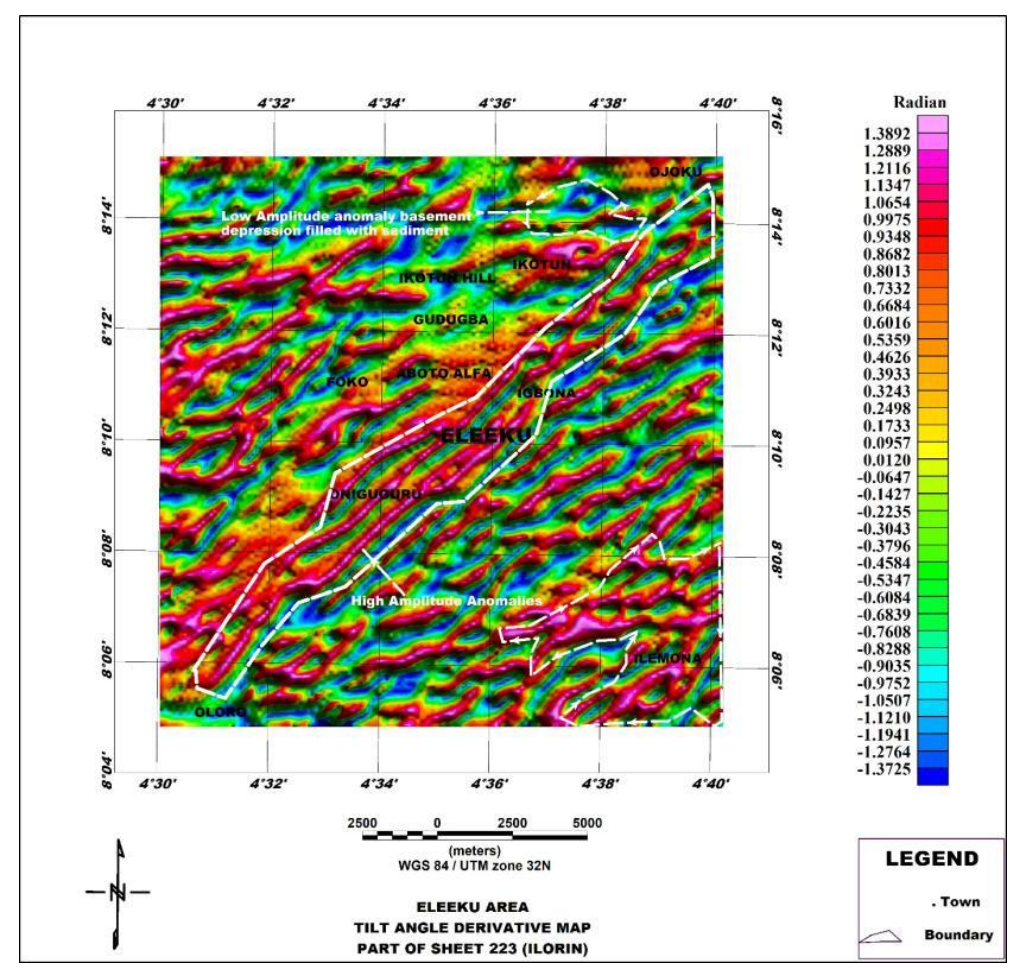


Figure 5: Color-Shaded TDR Map of Eleeku Area

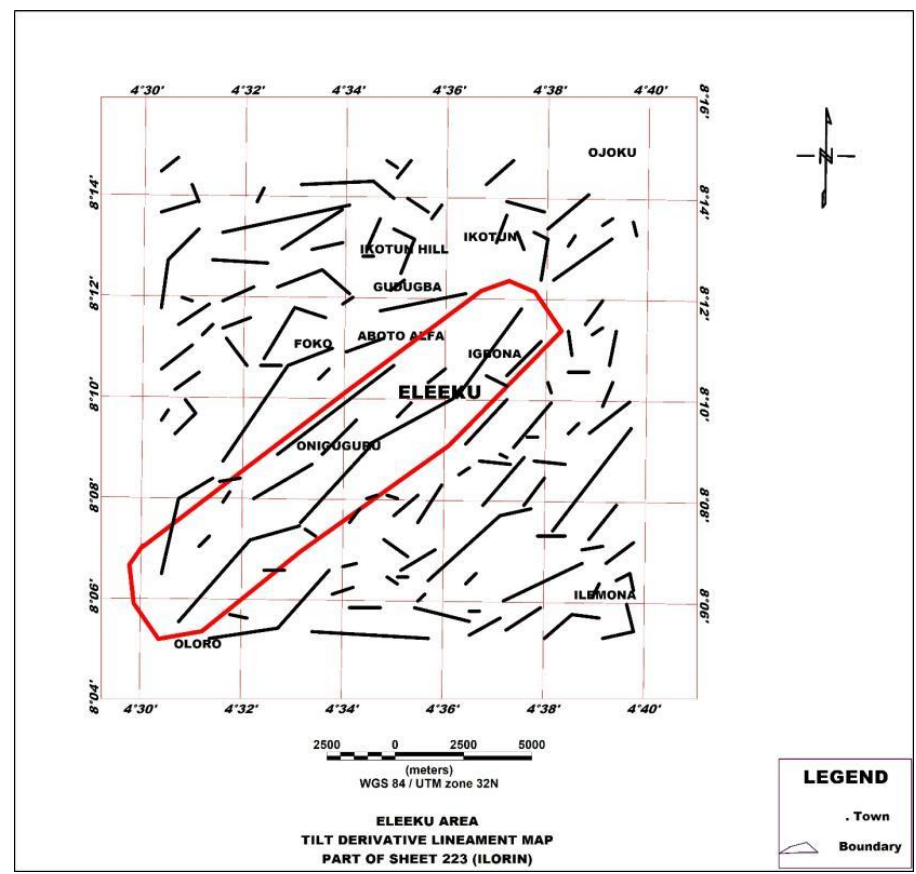


Figure 6: Lineaments Map of Eleeku Extracted from Color TDR

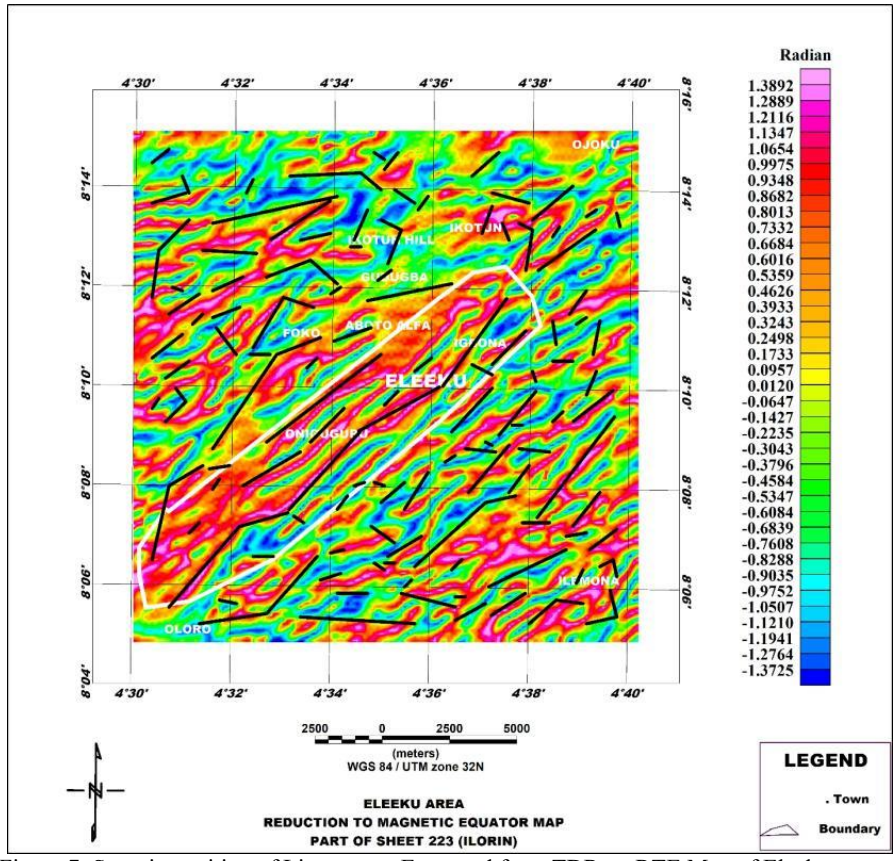


Figure 7: Superimposition of Lineaments Extracted from TDR on RTE Map of Eleeku

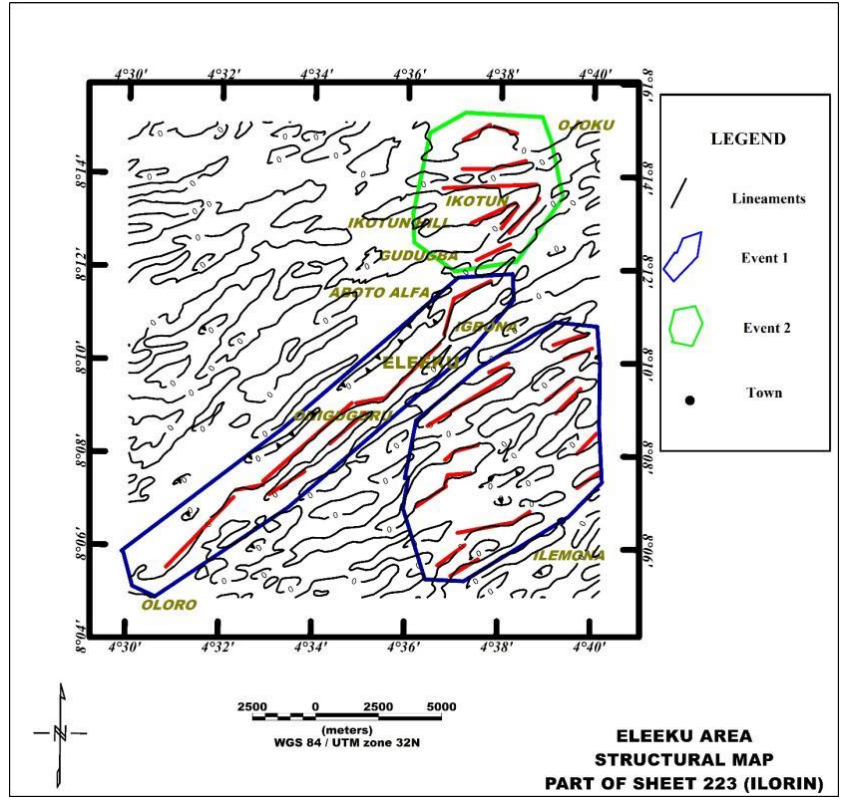


Figure 8: Superimposition of Maximum Point of HGM on TDR Zero Contour Lines Map of Eleeku

The elongated, linear peaks in the HGM-RTE anomaly delineate the boundaries of magnetic source entities. The HGM peaks are shown on the composite map (Figure 8) together with the TDR zero contour lines revealing a significant correlation between them for major structures in the anomaly signatures map. The structural complexity of the study area shown in Figure 9 (the composite map) revealed two major structural domains identified by variations in inferred lineament patterns with their spacing and orientation.

- Event 1 revealed that a major ductile deformation influenced the southwestern domain, resulting in NW– SE trends of interpreted contact and faults within the lithology of quartzite and muscovite schist that may possibly date back to the Eburnean era (pre- Pan-African) period
- ii. Event 2 showed that the eastern domain experienced a major ductile-brittle deformation, leading to notable trend of NE-SW direction in the unit rock of quartzite. These deformations were probably induced by tectonic activities related to Pan-African compression and prevailing temperature conditions.

3D-Euler Deconvolution

Figure 9 illustrates the result for a zero (0) structural index which corresponds to the magnetic contact model of the

depths range 50 to 1250 m. Some of these solutions representing contact zones between two different lithologies (i.e. igneous and sedimentary rocks) have been identified and highlighted on the map. A structural index of 0 for magnetic Euler deconvolution has been widely employed to delineate contacts between two lithologies (Nguyen et al., 2019). The map (Figure 9) highlights the contact between known pegmatite- rich zone at Eleeku community, believed to contain rare metals and gemstones and schist. This zone is of high magnetic signatures believe to be the magnetic properties of the host rock which generate the Earth's magnetic field anomalies that are discovered and identified from the surface influencing by the geological processes that also formed the rare earth element (REE)-rich pegmatites. Since the interested anomalies ranges between 4 to 6 km in width. About 6 km is estimated as the best size for window search and since the grid size which is about one-fourth of the line spacing is 100 m, then this corresponds to about 60 grid cells thereby it leads to specify 16 which is the maximum window size achievable in the 3D Euler deconvolution routine of Oasis Montaj software. These contact zones have been widely known for detection or exploration of minerals since it well known for hosting large quantity of minerals like garnet, tourmaline, mica and rocks like xenotliths (Paterson et al., 1991; Yaghoobian et al.,

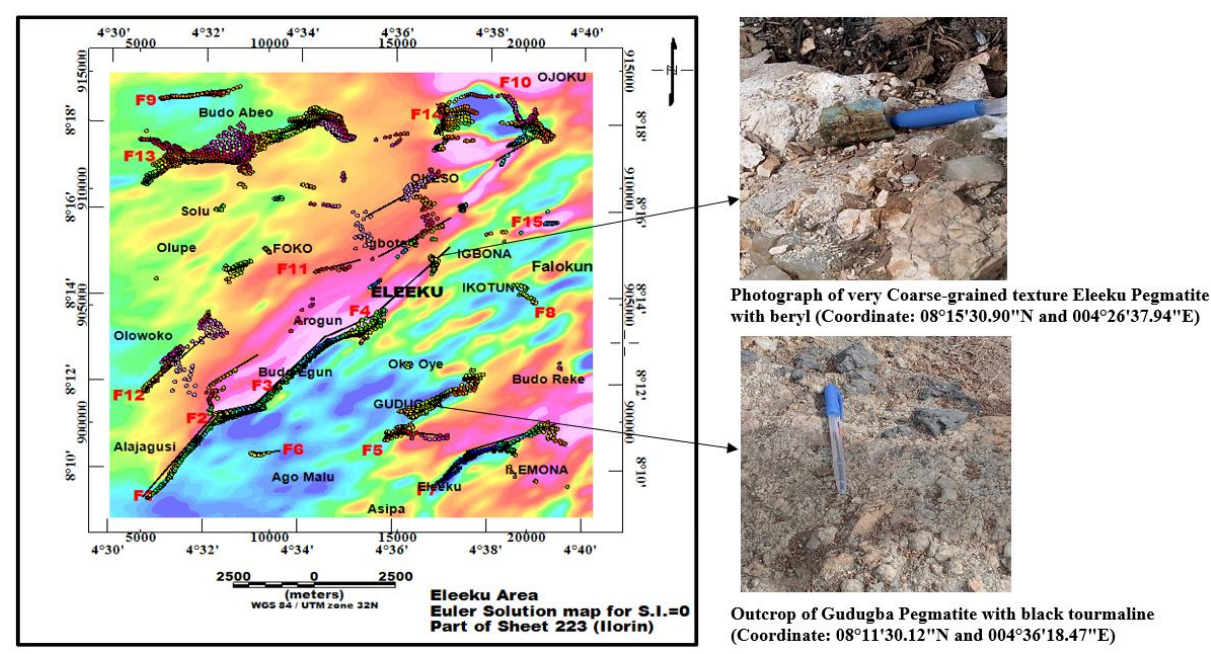


Figure 9: Euler Solution Plot of Eleeku Area for Windowed Solutions (SI = 0)

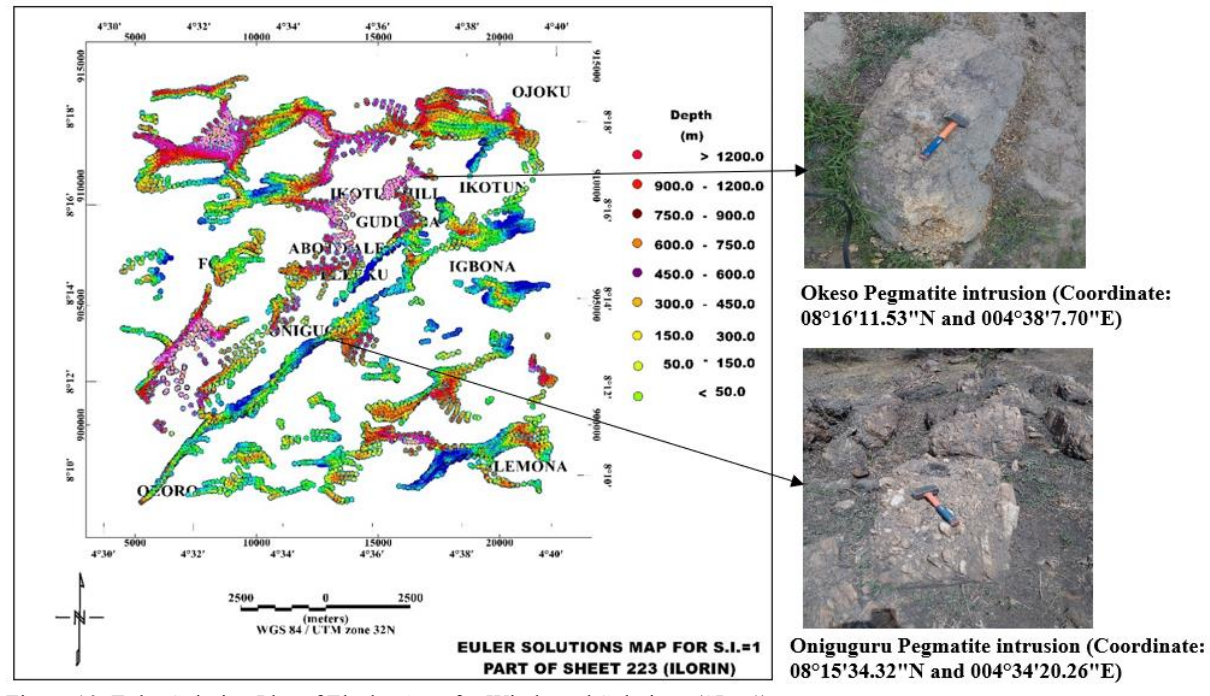


Figure 10: Euler Solution Plot of Eleeku Area for Windowed Solutions (SI = 1)

Figure 10 displays the structural index of sill/dyke model which is 1.0 with depths range of 50 to 1200 m. Here, the grid spacing was 100 m and the window size of 16 was equally chosen. The 3D Euler deconvolution structural index of 1.0 for sill/dyke has been used worldwide to detect dyke/sill (Yaghoobian *et al.*, 1992; Marchetti and Settimi 2011). The known rare metals and gemstone bearing pegmatite-rich zones in Eleeku, Ojoku and Okeso areas were demarcated for the purpose of correlation. Many of these contact and dyke structural features correlate with the known pegmatite-rich zones thereby confirming the association of structural indices 0.0 and 1.0 with muscovite rich areas.

Evaluation of the Dip Angle and Dip Direction for Various Faults

As previously discussed, the estimation of the depth of the field source was achieved through 3D Euler Deconvolution method with parameters of a 16x16 window size, a flight measurement of 80 metres and $\pm 15\%$ error. The structural index of 0 helped determine the depth and position of the source where the top of the anomaly boundary has a maximum depth of approximately 1200 metres. The Euler solution depth results are superimposed on the tilt angle zero value known as the Tilt and Euler map (Figure 11). This overlay reveals that the tilt angle zero contour align with the boundaries of anomalies. Four (4) classes of fault directions: longitudinal, latitudinal, Northwest-Southeast, and Northeast-Southwest were identified.

However, these 4 identified faults can be grouped as follow: -

- Longitudinal direction of 2 faults: Western part of Ojoku (F10) and Northern part of Ikotun (F14).
- Latitudinal and Sub-latitudinal direction of 6 faults. Western part of Ilemona (F5), Eastern part of Oloro (F6), Northwestern part of Ikotun Hill (F9), Southern part of Foko (F11), Northwestern part of Foko (F13) and Northeastern part of Igbona (F15).
- iii. NW-SE direction of 1 fault identified in the eastern region of Eleeku (F8).
- iv. NE-SW direction of 6 faults: Oloro (F1), Norteastern part of Oloro (F2), Southwestern part of Oniguguru (F3), Eleeku (F4), Southwestern part of Ilemona (F7) and Northern part of Oloro (F12).

Perpendicular lines were plotted and extracted at each fault which facilitated the determination of the dip angle and dip direction. The peak point of the THG on the measuring line was considered and the findings are shown in Table 2.

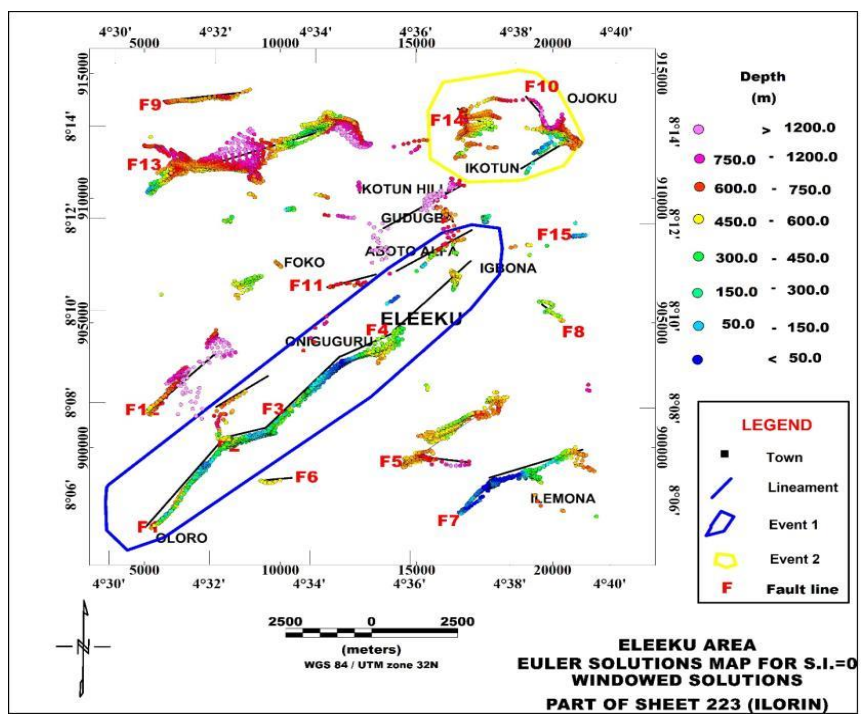


Figure 11: Superimposition of Peaks of HGM and Zero (0) Contour TDR on Euler Solution Plot of Eleeku Area

Table 2: The Features of Various Faults in the Study Area

S/N	Symbol	Direction of Fault	Direction of Dip	Dip Angle
1	F1	Northeast-Southwest	East	65 ⁰
2	F2	Northeast-Southwest	East	73 ⁰
3	F3	Northeast-Southwest	East	810
4	F4	Northeast-Southwest	East	64^{0}
5	F5	Latitudinal and Sub latitudinal	East	53^{0}
6	F6	Latitudinal and Sub latitudinal	East	210
7	F7	Northeast-Southwest	East	39^{0}
8	F8	Northwest-Southeast	East	18^{0}
9	F9	Latitudinal and Sub latitudinal	East	40^{0}
10	F10	Longitudinal and Sub longitudinal	East	53^{0}
11	F11	Latitudinal and Sub latitudinal	East	35^{0}
12	F12	Northeast-Southwest	East	59^{0}
13	F13	Latitudinal and Sub latitudinal	East	42^{0}
14	F14	Longitudinal and Sub longitudinal	East	47 ⁰
15	F15	Latitudinal and Sub latitudinal	East	56^{0}

CONCLUSION

This study characterized and determined the location, trend and depth of possible muscovite-bearing faults in Eleeku using 3-D Euler Deconvolution and Total Horizontal Gradient techniques of magnetic method. 15 major faults oriented in the NW-SE and NE-SW directions were discovered from the 3D Standard Euler and zero tilt derivative map were identified. 4 out of these 15 are carriers of muscovite bearing faults, with a maximum depth of approximately 600 m and

dip angles varying between 65° and 82° . 4 carriers of muscovite bearing faults out of 15 with a maximum depth range of 600 m and dip angles varying between 65° and 82° were determined. The maximum depths and dip angles to the top of the source bodies ranging between 450m - 1200m and 65° - 82° respectively were found in Gudugba and Aboto Alfa communities while the shallow source depths and dip angles ranges from 300 - 400 m and 18° – 64° were identified at Eleeku, Igbona and Oloro areas. fault with depths range of 50

m -600 m coincide with areas where muscovite-bearing faults were found within the outcropping basement rocks of Eleeku area at $(08^{\circ}\ 10'\ 26.06''N\ 004^{\circ}\ 35'\ 44.69''E)$ of high magnetic signatures. It is thereby recommended to carry-out ground truthing, geochemical analysis or integration of other geophysical methods like radiometric, gravity or electrical resistivity to follow-up the results.

REFERENCES

Adekoya, J. A., Kehinde-Phillips, O. O., & Odukoya, A. M. (2003). Geological distribution of mineral resources in Southwestern Nigeria. In A. A. Elueze (Ed.), *Prospects for investment in mineral resources of Southwestern Nigeria* (pp. 15–56). Nigerian Mining and Geosciences Society (NMGS).

Ajibade, A. C., Woakes, M., & Rahaman, M. (1987). Proterozoic crustal development in the Pan-African regime of Nigeria. In A. Kroner (Ed.), *Proterozoic lithospheric evolution* (pp. 259–271). American Geophysical Union.

Aliyu, A., Lawal, K., Abubakar, I. Y., Wada, A., & Olayinka, A. L. (2020). Geomagnetic studies of pegmatite mineralisation at Lema and Ndeji North-Central, Nigeria. *Journal of Mining and Geology*, 56(1), 81–89.

Balogun, O. B. (2019). Tectonic and structural analysis of the Migmatite–Gneiss–Quartzite complex of Ilorin area from aeromagnetic data. *NRIAG Journal of Astronomy and Geophysics*, 8(1), 22–33. https://doi.org/10.1080/20909977.2019.1615795

Barbosa, V., Sliva, J., & Medeiros, W. (1990). Stability analysis and improvement of structural index in Euler deconvolution. *Geophysics*, 64, 48–60.

Bassey, N., & Barka, J. (2015). Lithologic and structural mapping using aeromagnetic and ground radiometric data in Song Area, N. E. Nigeria. *Journal of Geography, Environment and Earth Science International*, *2*(4), 173–179. https://doi.org/10.9734/jgeesi/2015/18085

Bassey, R. (2011). *Interpretations of aeromagnetic data from Ilesha* (pp. 1–92).

Blakely, R. J., & Simpson, R. W. (1986). Approximating edges of source bodies from magnetic or gravity anomalies. *Geophysics*, *51*(7), 1494–1498.

Chiapkin, K. F. (1969). The analysis of gravity data in the study of deep crust structure. Vnigeophizika.

Cordell, L., & Grauch, V. J. S. (1985). Mapping basement magnetization zones from aeromagnetic data in the San Juan Basin, New Mexico. In W. J. Hinze (Ed.), *The utility of regional gravity and magnetic anomaly maps* (pp. 181–197). Society of Exploration Geophysicists.

Dada, S. S. (1998). Crust-forming ages and Proterozoic crustal evolution in Nigeria: A reappraisal of current interpretations. *Precambrian Research*, 87(1), 65–74.

Durrheim, R. J., & Cooper, G. R. J. (1998). Euldep, a program for the Euler deconvolution of magnetic and gravity data. *Computers & Geosciences*, 24(6), 545–550.

Garba, I. (2003). Geochemical discrimination of newly discovered rare metal bearing and barren pegmatites in the

Pan-African (600 ± 150 Ma) basement of Northern Nigeria. Applied Earth Science Transactions of the Institute of Mining and Metallurgy, 112, B287–B291. https://doi.org/10.1179/037174503225011270

Ibrahim, A. A., & Hayatu, R. A. (2021). Genesis and rare metal potential of pegmatites around Makarfi area, North Western Nigeria. *Journal of African Earth Sciences*, 178, 104183. https://doi.org/10.1016/j.jafrearsci.2021.104183

Ishola, K. S., Akerele, P. O., Folarin, O., Adeoti, L., Adegbola, R. B., & Adeogun, O. Y. (2020). Application of aeromagnetic data to map subsurface structural features in Ewekoro, Southwestern Nigeria. *Modeling Earth Systems and Environment*, 6(4), 2291–2302. https://doi.org/10.1007/s40808-020-00812-y

Lawal, T. O. (2020). Integrated aeromagnetic and aeroradiometric data for delineating lithologies, structures, and hydrothermal alteration zones in part of southwestern Nigeria. *Arabian Journal of Geosciences*, 13(16). https://doi.org/10.1007/s12517-020-05743-7

Li, X. (2008). Magnetic reduction-to-the-pole at low latitudes: Observations and considerations. *The Leading Edge, 27*(8), 990–1002.

Magaji, Y., & Sanusi, Y. A. (2021). Evaluation of hydrocarbon prospect in Lema area, western parts of Sokoto Basin, Nigeria, based on analysis of high-resolution aeromagnetic data. *Quest Journals Journal of Research in Environmental and Earth Sciences*, 7(4), 46–61.

Marchetti, M., & Settimi, A. (2011). Integrated geophysical measurements on a test site for detection of buried steel drums. *Annals of Geophysics*, 54(1), 105–114.

McCurry, P. (1978). Geology of degree sheets 19 (Zuru), 20 (Chafe), and part of 19 (Katsina). In *Overseas Geological Mineral Resource, Nigeria* (p. 53).

Miller, H. G., & Singh, V. (1994). Potential field tilt: A new concept for location of potential field sources. *Journal of Applied Geophysics*, 32, 213–217.

Mushayandebvu, M., van Driel, P., Reid, A., & Fairhead, J. (2001). Magnetic source parameters of two-dimensional structures using extended Euler deconvolution. *Geophysics*, 66(3), 814–823.

Nabighian, M. N. (1972). The analytic signal of two-dimensional magnetic bodies with polygonal cross-section: Its properties and use for automated anomaly interpretation. *Geophysics*, *37*, 507–517. https://doi.org/10.1190/1.1440276

NGSA. (2023). LITHO-STRUCTURAL MAP OF NIGERIA. *Nigeria Geological Survey Agency*. https://ngsa.gov.ng/litho-structural-map-of-nigeria/

Nguyen, H. H., Dang, L. V., & Vo, V. V. (2019). A combined Euler deconvolution and tilt angle method for interpretation of magnetic data in the South region. *Science and Technology Development Journal*, 22(2), 219–227. https://doi.org/10.32508/stdj.v22i2.1226

Okunlola, O. A., & Jimba, S. (2006). Compositional trends in relation to Ta-Nb mineralisation in Precambrian pegmatites

of Aramoko-Ara-Ijero area, Southwestern Nigeria. *Journal of Mining and Geology*, 42(2), 113–126.

Okunlola, O. A., & Ogedengbe, O. (2003). Investment potential of gemstone occurrences in Southwestern Nigeria. In A. A. Elueze (Ed.), *Prospects for investment in mineral resources of Southwestern Nigeria* (pp. 41–45). Nigerian Mining and Geosciences Society (NMGS).

Okunlola, O. A., & Ofonime, B. E. (2006). Geological setting, petrographical features and age of rare metal (Ta-Nb) mineralisation of pegmatite of Komu area, Southwestern Nigeria. *African Journal of Science and Technology*, 7(1), 96–110.

Okunlola, O. A. (2005). Metallogeny of Tantalum-Niobium mineralisation of Precambrian pegmatites of Nigeria. *Mineral Wealth*, *137*, 38–50.

Olaoluwa, D. T., Abdulmalik, A. E., Muraina, T. A., Girigisu, S., & Balogun, A. F. (2020). Dissolution of a Nigerian sourced muscovite ore for use as an ingredient in paint production. *Journal of the Nigerian Society of Physical Sciences*, 2(3), 128–133. https://doi.org/10.46481/jnsps.2020.89

Oladejo, O. P., Adagunodo, T. A., Sunmonu, L. A., Adabanija, M. A., Enemuwe, C. A., & Isibor, P. O. (2020). Aeromagnetic mapping of fault architecture along Lagos-Ore axis, Southwestern Nigeria. *Open Geosciences*, 12(1), 376–389. https://doi.org/10.1515/geo-2020-0100

Olayinka, L. A., Ahmed, A. L., Lawal, K. M., & Muhyideen, H. (2019). Application of electrical resistivity imaging and induced polarization methods for groundwater exploration at Ahmadu Bello University phase ii, Zaria, Nigeria. *FUDMA Journal of Sciences (FJS)*, 3(3), 123–130.

Oluyide, P. O., Nwajide, C. S., & Oni, A. O. (1988). The geology of Ilorin area. *Bulletin Geological Survey of Nigeria*, 42, 60–66.

Osagie, A. U., Eshanibli, A., & Adepelumi, A. A. (2021). Structural trends and basement depths across Nigeria from analysis of aeromagnetic data. *Journal of African Earth Sciences*, 178, 104184. https://doi.org/10.1016/j.jafrearsci.2021.104184

Oyawoye, M. (1972). The basement complex of Nigeria. In T. F. J. Dessauvagie & A. J. Whiteman (Eds.), *African geology* (pp. 66–102). Ibadan University Press.

Paterson, N. R., Kwan, K. C. H., & Reford, S. W. (1991). Use of Euler deconvolution in recognizing magnetic anomalies of pipelike bodies. In *Proceedings of the SEG Annual Meeting, Houston* (pp. 642–645).

Phillips, J. D. (2000). Locating magnetic contacts: A comparison of the horizontal gradient, analytic signal, and local wavenumber methods. In *SEG Technical Program Expanded Abstracts* 2000 (pp. 402–405). Society of Exploration Geophysicists.

Rahaman, M. A. (1988). Recent advances in the study of the Basement Complex of Nigeria. In *Precambrian geology of Nigeria* (pp. 11–43). Geological Survey of Nigeria.

Rahaman, M. A. (1989). Review of basement geology of Southwestern Nigeria. In C. A. Kogbe (Ed.), *Geology of Nigeria* (2nd ed., pp. 39–56). Rock View Ltd.

Ravat, D. (1996). Use of magnetic data in geothermal studies.

Reid, A. B., Allsop, J. M., Granser, H., Millet, A. J., & Somerton, I. (1990). Magnetic interpretation in three dimensions using Euler deconvolution. *Geosciences Research*, 55, 80–91.

Roest, W. R., & Pilkington, M. (1993). Identifying remanent magnetization effects in magnetic data. *Geophysics*, *58*, 653–659.

Roest, W. R., Verhoef, J., & Pilkington, M. (1992). Magnetic interpretation using the 3-D analytic signal. *Geophysics*, 57(1), 116–125.

Salaudeen, S. A., Adagunodo, T. A., Busari, A. O., Suleman, K. O., & Sunmonu, L. A. (2025). Depth estimation of the residual field of Patigi Area, Nigeria, using source parameter imaging and spectral depth analysis. *Recent Advances in Natural Sciences Journal*, 3, 1–7. https://doi.org/10.61298/rans.2025.3.1.210

Salem, A., Williams, S., Fairhead, J., Ravat, D., & Smith, R. (2007). Tilt depth method: A simple depth estimation method using first-order magnetic derivatives. *The Leading Edge*, *26*, 1502–1505.

Sherif, S. D. (2010). Matched filter separation of magnetic anomalies caused by scattered surface debris at archaeological sites. *Near Surface Geophysics*, 8, 145–150.

Thompson, D. T. (1982). EULDPH – A new technique for making computer-assisted depth estimates from magnetic data. *Geophysics*, 47, 31–37.

Turner, D. (1983). Upper Proterozoic schist belts in the Nigerian sector of the Pan-African province of West Africa. *Precambrian Research*, 21(1–2), 55–79.

Usman, N., Lawal, K. M., & Aku, M. O. (2014). Application of Werner deconvolution method in the direct interpretation of residual aeromagnetic anomalies. *IOSR Journal of Applied Physics*, *6*(1), 18–21. https://doi.org/10.9790/4861-06131821

Verduzco, B., Fairhead, J. D., Green, C. M., & MacKenzie, C. (2004). New insights into magnetic derivatives for structural mapping. *The Leading Edge*, 23, 116–119.

Whitehead, N., & Musselman, C. (2008). Montaj Grav/Mag interpretation: Processing, analysis and visualisation systems for 3D inversion of potential field data for Oasis Montaj v6.3. Geosoft Incorporated.

Yaghoobian, A., Boustead, G. A., & Dobush, T. M. (1992). Object delineation using Euler's homogeneity equation. In *Proceedings of SAGEEP 92, San Diego, California*.



©2025 This is an Open Access article distributed under the terms of the Creative Commons Attribution 4.0 International license viewed via https://creativecommons.org/licenses/by/4.0/ which permits unrestricted use, distribution, and reproduction in any medium, provided the original work is cited appropriately.